Rationalizing the role of structural motif and underlying electronic structure in the finite temperature behavior of atomic clusters

Anju Susan and Kavita Joshi

Citation: The Journal of Chemical Physics **140**, 154307 (2014); doi: 10.1063/1.4871118
View online: http://dx.doi.org/10.1063/1.4871118
View Table of Contents: http://scitation.aip.org/content/aip/journal/jcp/140/15?ver=pdfcov
Published by the AIP Publishing

Rationalizing the role of structural motif and underlying electronic structure in the finite temperature behavior of atomic clusters

Anju Susan and Kavita Joshi
Center of Excellence in Scientific Computing and Physical and Materials Chemistry Division, CSIR-National Chemical Laboratory, Pune 411008, India

(Received 22 July 2013; accepted 1 April 2014; published online 18 April 2014)

Melting in finite size systems is an interesting but complex phenomenon. Many factors affect melting and owing to their interdependencies it is a challenging task to rationalize their roles in the phase transition. In this work, we demonstrate how structural motif of the ground state influences melting transition in small clusters. Here, we report a case with clusters of aluminum and gallium having same number of atoms, valence electrons, and similar structural motif of the ground state but drastically different melting temperatures. We have employed Born-Oppenheimer molecular dynamics to simulate the solid-like to liquid-like transition in these clusters. Our simulations have reproduced the experimental trends fairly well. Further, the detailed analysis of isomers has brought out the role of the ground state structure and underlying electronic structure in the finite temperature behavior of these clusters. For both clusters, isomers accessible before cluster melts have striking similarities and does have strong influence of the structural motif of the ground state. Further, the shape of the heat capacity curve is similar in both the cases but the transition is more spread over for Al_{36} which is consistent with the observed isomerization pattern. Our simulations also suggest a way to characterize transition region on the basis of accessibility of the ground state at a specific temperature.
 [http://dx.doi.org/10.1063/1.4871118]

I. INTRODUCTION

Melting is a first order phase transition in bulk. In finite size systems, it is still a puzzle especially in the region where *each atom counts*. Not just the order of the transition could be different,[1] but finiteness of the system also gives rise to many other interesting processes such as dynamical coexistence,[2–4] premelting, and post-melting.[5–9] The transition is highly size sensitive and clusters of same element show huge variety in the way they undergo this transition.[10–16] The observed variation is most drastic and dramatic in the systems with few tens of atoms. While it is now accepted that clusters with even few tens of atoms undergo phase transition, the contribution of different factors determining the nature of transition is not yet completely understood. Two generic features are observed in all the experiments done so far (i) considerable variation in the melting temperatures (T_m) as a function of size of the cluster and (ii) size sensitive shape of the heat capacity curve. Focus of all the recent simulations has been towards understanding the factors responsible for such variations.[17–40]

The heat capacity curve of a cluster is characterized by two features, the peak and the shape. Peak in the heat capacity curve is considered as the melting temperature of the system whereas the shape of the heat capacity curve represents the nature of transition. Simulations have revealed that the Ground State (GS) geometry is a decisive element in determining the melting temperature as well as shape of the heat capacity curve.[17–26,41] For example, in case of sodium clusters, a depression in the melting temperature is observed around size 92. Na_{55} and Na_{142} melt at 290 K and 270 K, respectively, whereas T_m of Na_{92} is around 210 K.[11] Simulations revealed that the ground state geometries of 55 and 142 atom clusters have icosahedral structural motif while the GS for 92 atom cluster deviates from the icosahedral motif leading to a relatively low T_m.[19,20] In case of Aluminum, the T_m varies between 450 K and 850 K, for clusters with 16–48 atoms.[16] Changes in the structural motif of the GS appear to be mainly responsible for the large variations observed in the melting temperatures.[17] Gallium clusters in the size range 30–55 have elevated melting temperatures.[13,14] It was argued that change in the nature of bonding is responsible for higher than bulk melting temperatures.[21] Another interesting feature observed is variation in the melting temperature as a function of cluster size. Clusters with 30–39 atoms melt between 500 K and 600 K whereas larger clusters (around size 48) have their T_m near 800 K, substantially higher than clusters with few atoms less. It was demonstrated that structural motif of the GS is crucial in determining finite temperature behavior of these clusters.[22] Emergence of spherical structures as the ground state leads to higher melting temperatures. Enhanced stability of the spherical GS is due to the well separated core and surface shells, which consequently delays isomerization.[22]

Structural motif of the GS also plays a key role in determining shape of the heat capacity curve. For example, clusters with a distinguishable peak in the heat capacity curve have ordered ground state structure.[24] A rationale behind this is as follows. An ordered system is the one where most of the constituent atoms are equivalent and experience similar environment resulting into a very much alike response to the external stimulus like temperature. Contrary to this, a disordered GS will be the one having many atoms with different surrounding, which will also reflect in their distinct response to the change in the external conditions. Al_{44} with an "ordered" GS exhibits sharpest peak in the whole range

explored experimentally.[16,17] A similar relation between the GS structure and shape of the heat capacity curve has been predicted and/or demonstrated by *ab initio* molecular dynamics simulations for clusters of Na and Ga.[23,24] Vacancies also play a crucial role in determining the shape of the heat capacity curve. Au_{20} with tetrahedral structure exhibits a peak in the heat capacity curve, whereas Au_{19}, with one missing apex atom, leads to a phase transition spread over a range of temperatures resulting into a broad peak in the heat capacity curve.[25] Ghazi *et al.* demonstrated the effect of electronic structure and charge state on the thermodynamic properties of Na clusters.[26] They observed that addition of even one electron increases the melting temperature by 40 K with sharper heat capacity curve for certain sizes.[26] In case of Al clusters, significant variation in T_m was observed for cations and anions, specifically for sizes near structural transition.[17] Recently, Aguado and López have investigated effect of electronic shell and charge state on melting of Al clusters.[18]

Even if it has been demonstrated that change in the structural motif of the GS and variation in the melting temperature are correlated, the picture is not yet clear. With size of the cluster, not only the structural motif of the GS changes, but also other factors influencing melting transition like underlying electronic structure, isomer distribution, surface energy, "order/disorder" of the structure vary. These factors have complex interdependencies and it is difficult to separate effect of one factor from the other. A change in the structure also changes the underlying electronic structure, the coordination of atoms within the cluster, "order" in the cluster which in turn reflects in the environment that an atom experiences within a cluster. Thus, even a small variation like addition or removal of a single atom from a cluster results into completely different finite temperature behavior not only in terms of melting temperature but also in the transition pattern. To rationalize the role of various factors one would like to have a system with as many similarities as possible. Al_{36} and Ga_{36} are one such case where structural motif of the ground state and the number of valence electrons, the two most important factors are same with drastically different melting temperatures.

Although at finite size Al and Ga have more similarities than differences, in bulk form, these elements have distinctly different properties. Bulk gallium is known for its polymorphism. There are many stable phases of gallium, α-Ga being the most stable at ambient conditions. The lattice structure of α-Ga can be viewed as base-centered orthorhombic with eight atoms in the unit cell.[42] Each atom has one short bond at a distance 2.44 Å and six other neighbors at distances of 2.71 Å and 2.79 Å, in two sets of three.[42] These six atoms form buckled parallel planes connected via the shortest bond. The electronic structure calculations reveal that the shortest bond is covalent in nature whereas the bonding in the buckled planes leads to an observed metallic behavior. The lattice structure of Al is face centered cubic crystal with s-p hybridized valence band. In bulk form, Al and Ga melt at 933 K and 303 K, respectively. However, clusters of gallium in the size range 30–50 have elevated melting temperatures and melt between 400 K and 900 K, same as that of Al clusters.[13–15] Interestingly, clusters of both the elements have similar growth pattern.[41,43] Up to size 5 these clusters have similar structural motif of the GS. For larger clusters, around 18 to 23, appearance of stacking sequences including five- and six-membered ring is observed for Al as well as Ga. Around 36, the structural motif of the GS shows dominance of layer formation in both cases.[22,41]

In spite of having similar trends in the structural motif of the GS and overall range of melting temperatures, the specific pattern varies considerably. For example, for both the elements, the GS of clusters with 30–40 atoms is dominated by layered structures. But the finite temperature behavior of these clusters differs substantially. The melting temperature as a function of cluster size, peaks at 850 K for Al_{37} whereas for Ga, T_m fluctuates between 500 K and 600 K in this size range. In case of gallium, 31, 33, 36, and 37 are "melters" with distinct peak in the heat capacity curve. For aluminum, up to 34, all clusters are "non-melters," i.e., without a distinguishable peak in the heat capacity curve. This points out the fact that melting transition in small clusters is a complex phenomenon and does depend on many factors. On this background, to rationalize the effect of GS geometry on the solid-like to liquid-like transition, Al_{36} and Ga_{36} clusters provide a unique opportunity. Note that these two clusters have similar structural motif of the GS and same number of valence electrons but drastically different melting temperatures. Specifically, we would like to investigate how the structural motif of the GS influences the solid-like to liquid-like transition and what is the effect of underlying electronic structure on the same. In what follows we will demonstrate the similarities in the structural motif of GS, variation in the bonding due to the different underlying electronic structures and their effect on the phase transition. In Sec. II, the computational details and other qualitative parameters used to analyze the data are discussed. The results are presented in Sec. III with the discussion, and the conclusions are drawn in Sec. IV.

II. COMPUTATIONAL DETAILS

To reproduce the observed experimental data, Density Functional Theory (DFT) level treatment of valence electrons is indispensable. We have employed Born-Oppenheimer molecular dynamics simulations as implemented in Vienna *Ab initio* Simulation Package (VASP).[44–47] The Projector Augmented Wave (PAW) method which generalizes both the pseudo potential method and the linear augmented-plane-wave method, with Perdew-Burke-Ernzerhof (PBE) exchange correlation functional[48,49] has been used for both Al and Ga. The energy cutoff for each self-consistency iteration was kept at 10^{-4} eV. A fairly good guess for the global minima is important because although the melting temperature does not depend on the starting point, the premelting behavior will be affected by the starting geometry. Various groups have reported GS of Al_{36}[17,18,40,50] and Ga_{36}[22,41] by employing different methods like basin hopping, optimizing bulk fragments, selective optimization of geometries picked from a high temperature melt, etc. All of them have reported the same structure as the global minima which is a distorted decahedral fragment (ddf). Our extensive search also confirms the same structure for both the systems.

The finite temperature behavior of these clusters was simulated by employing Nośe thermostat. Starting from the ground state structure, the clusters were heated slowly with heating rate of 100 K/30 ps to a specific temperature. Then the clusters were maintained at that temperature for at least 150 ps. For temperatures in the transition region, the simulation time was more than 400 ps. A total of 18 temperatures were simulated for Ga_{36} between 100 K and 900 K and 19 temperatures for Al_{36} between 100 K and 1200 K, resulting into total simulation time of about 3.8 ns or more for each system. The heat capacity curve was obtained by employing multiple histogram technique which permits better estimation of the classical density of states. A detailed account of this technique could be found in Refs. 51 and 52. The finite temperature data were also analyzed using qualitative parameters like root mean square bond length fluctuations ($\delta_{\rm rms}$), mean square displacements, distance of atoms from Center Of Mass (COM) of the cluster, and potential energy distribution as a function of temperature.

As the name suggests, $\delta_{\rm rms}$ is a measure of fluctuations in the bond-lengths averaged over all atoms and total time span. It is defined as

$$\delta_{\rm rms} = \frac{2}{N(N-1)} \sum_{i>j} \frac{\left(\langle r_{ij}^2 \rangle_t - \langle r_{ij} \rangle_t^2\right)^{1/2}}{\langle r_{ij} \rangle_t}, \qquad (1)$$

where N is the number of particles in the system, r_{ij} is the distance between particle i and j, and $\langle \ldots \rangle_t$ denotes a time average over the entire trajectory. According to the Lindemann criteria when value of δ_{rms} exceeds 0.1 the system is melted. For clusters, at low temperatures, the δ_{rms} rises linearly indicating that the amplitude of oscillations is increasing with temperature. The isomerization is marked by δ_{rms} crossing 0.1. However, for clusters, it has been observed that the value of δ_{rms} saturates about 0.25 to 0.3 when the system is in liquid like state.

III. RESULTS AND DISCUSSION

We begin the discussion by comparing the ground state geometries and the underlying electronic structure for both clusters. Figure 1 brings out similarities in the structural motif and differences in the nature of bonding and connectivity of these two structures. The structural motif of the GS is distorted decahedral fragment (D_{2d}) which is shown in Fig. 1(a). The distance of atoms from the COM of the cluster, shown in Fig. 1(b), confirms that both the clusters have identical structural motif. In order to bring out the difference in the nature of bonding, the number of bonds with bond-length less than 2.8 Å was calculated and is shown in Fig. 1(c). In bulk, the coordination number is computed by taking the bond-length cutoff as the first minima in pair distribution function (3.8 Å for Ga). However, when the size of the system is finite, it is more appropriate to take a smaller cutoff. In this work, the choice of a proper cutoff was made by investigating the charge density distribution along the line joining two atoms, as a function of distance between the atoms (from 2.6 Å, i.e., dimer bond length to 3.8 Å). It is found that up to 2.8 Å, the maximum charge density lies between two

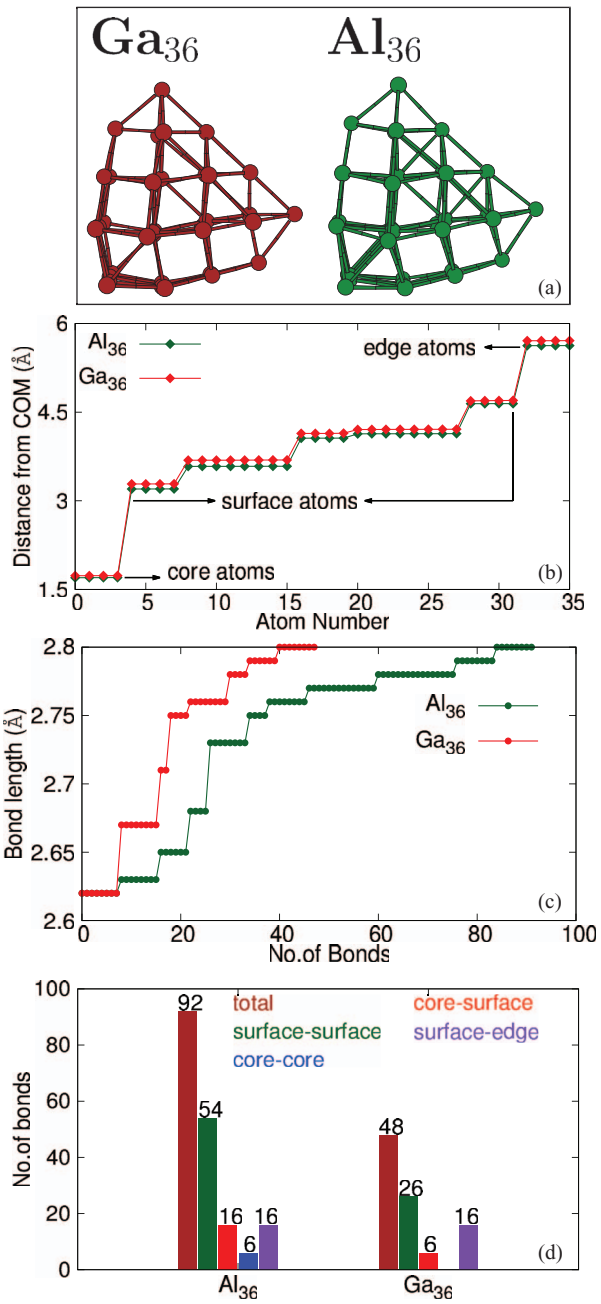

FIG. 1. (a) The ground state structure of Ga_{36} and Al_{36}; (b) distance from the center of mass the cluster; (c) number of bonds with bond-length less than 2.8 Å, and (d) connectivity between different shells as well as within shell with cutoff as 2.8 Å. Note that in spite of similar structural motif for the GS, the bonding and connectivity are drastically different.

atoms. When the separation is increased further (>2.8 Å), the charge distribution peaks at atomic sites rather than along the bond. Interestingly, although both clusters have their shortest bond-length of the same order, Al_{36} has 92 bonds with bond length less than 2.8 Å, whereas Ga_{36} has only 48 bonds (see Fig. 1(c)). This implies that for Al_{36}, the average number of bonds per atom is about 2.5, whereas for Ga_{36} it is around 1.3. Further difference is brought out by investigating distribution of these bonds among different shells of the cluster. For both systems, all the atoms are divided into three shells. The first shell (nearest to the COM of the cluster) consists of the inner most four atoms. The next shell includes four sub-shells with

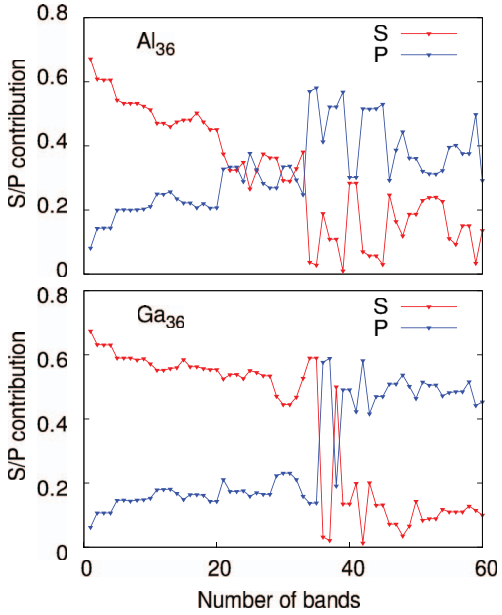

FIG. 2. Site projected wave function character of each molecular orbital for Al_{36} and Ga_{36}. The difference in the underlying electronic structure is very clear. For Al_{36} s-p hybridization set in around 22 whereas for Ga_{36} there is no signature of hybridization.

a total of 28 atoms, which forms the surface of the cluster and the outer most shell is made of four edge atoms. In Al_{36}, atoms within the same shell as well as from different shells are well connected, which is evident from the non zero value of core-core, core-surface, surface-surface, and edge-surface connectivity shown in Fig. 1(d). On the contrary, for Ga_{36}, most of the shortest bonds reside on the surface with very little connectivity among the core and the surface atoms and no connectivity within the core shell.

To bring out the difference in the underlying electronic structure, in Fig. 2, we show the site projected wave function character of each Molecular Orbital (MO) which is calculated by projecting the wave-functions onto spherical harmonic. The detailed investigation of MOs for both the systems reveals interesting information. For Al_{36}, the sp hybridization sets in very early at 22nd MO, but not all the MOs after 22 are hybridized. In case of Ga_{36}, the hybridization is not very prominent, and the detailed analysis of MOs reveal that, the first 15 MOs with atomic "s" as a dominant component clearly follow Jellium like pattern. However, rest of the MOs which are formed out of atomic "s" as well as atomic "p" do not adhere to the Jellium model very clearly. Out of 54 MOs, both the systems have about 20 MOs similar in character. In short, although the GS of Al_{36} and Ga_{36} has identical structural motif, the underlying electronic structure and resulting bonding is significantly different. In what follows, we bring out effects of "same structural motif with substantially different nature of bonding" on the *solid-like* to *liquid-like* transition of these two clusters.

Next, we compare the finite temperature behavior of these two clusters. In Fig. 3, we show the canonical heat capacity, averaged HOMO-LUMO gap, and the δ_{rms} as a function of temperature. Note that the peak in the heat capacity curve (see Fig. 3(a)) which is identified as the melting tem-

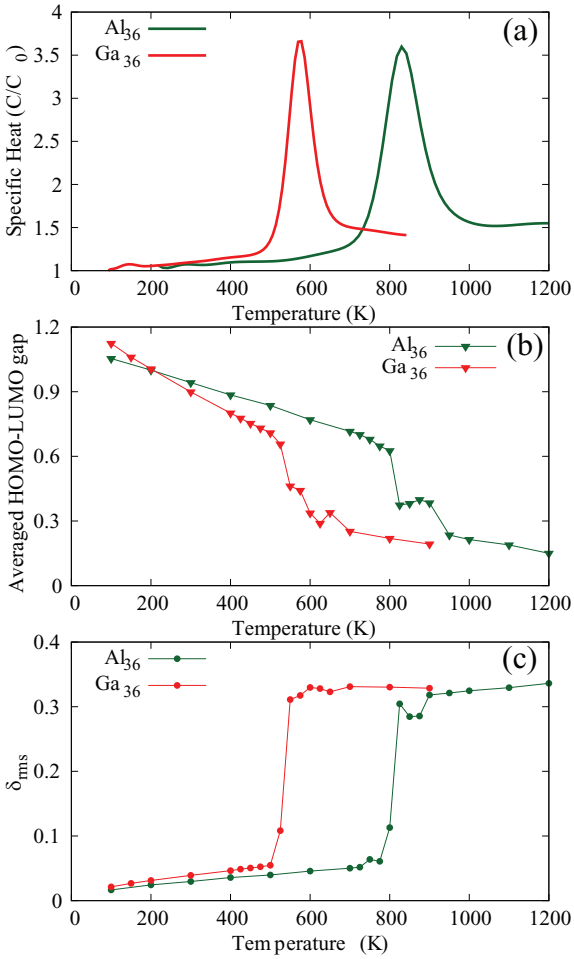

FIG. 3. (a) Heat capacity curve; (b) averaged HOMO-LUMO gap; and (c) δ_{rms} for Ga_{36} and Al_{36} as a function of temperature.

perature indicates that Ga_{36} melts around 580 K whereas T_m for Al_{36} is 830 K. The experimentally measured melting temperatures for Ga_{36}^+ and Al_{36}^+ are 525 K and 834 K, respectively, indicating that our simulations have reproduced experimental trend fairly well. We also note that the transition is slightly broader for Al_{36}. This will be more evident with isomer analysis which is presented later. The averaged HOMO-LUMO gap (see Fig. 3(b)) decreases marginally and monotonically in the solid like region. However, with the isomerization setting in, the gap decreases rapidly and is steeper in Ga_{36} than Al_{36}. For Ga_{36} till 500 K, 54th orbital is HOMO and 55th orbital is LUMO. At 525 K, with on set of isomerization, for a small fraction of instances (less than 1%), LUMO is shifted to 56th orbital. However, at higher temperatures, there are increasing instances where 54th and 55th orbitals become degenerate and 56th orbital is LUMO. For Ga_{36}, at 800 K 26% of times LUMO is shifted to 56th orbital. We have also noticed that, very few times (less than 1%) 54th, 55th, and 56th orbitals are degenerate with 57th orbital as LUMO. In case of Al_{36}, before isomerization sets in, i.e., up to 725 K, HOMO is 54th orbital and LUMO is 55th orbital. With isomerization, for a small fraction of instances (less than 1%), LUMO is shifted to 56th orbital. This fraction increases at higher temperatures. For example, 41% of times LUMO is located at 56th orbital for Al_{36} at 1100 K. Further, the degeneracy between 54th,

55th, and 56th orbitals was observed with marginally more probability (more than 1%). This is reflected in the averaged HOMO-LUMO gap as shown in the Fig. 3(b). The variation in the HOMO-LUMO gap at a specific temperature associates well with the isomerization pattern observed at that temperature. Figure 3(c) shows the δ_{rms} averaged over 120 ps for each temperature, except for transition region where the averages are taken over 400 ps. In the solid-like region ions are oscillating about their mean positions and with rise in temperature the amplitude of oscillations increases, which is reflected as a monotonic increment in the value of δ_{rms}. A sharp rise is seen after 800 K and 525 K for Al_{36} and Ga_{36}, respectively. With isomerization setting in at these temperatures, δ_{rms} exceeds 0.1. However, unlike bulk, for clusters value of δ_{rms} more than 0.1 does not always signal melting transition, in fact it is an indicator of isomerization. In a liquid like region and solid like region, δ_{rms} increases linearly with temperature but with a different slope. However, in the transition region, the δ_{rms} fluctuates. In short, both the systems have striking similarity in the nature of heat capacity curve as well as δ_{rms}. However, the transition temperatures are substantially different for these systems.

To shed more light on the way GS influences the melting transition, we have done extensive isomer analysis. From each finite temperature MD run we have selected at least 50 initial geometries (equally spaced, unbiased) and carried out local optimizations. For transition region, the number of local optimizations carried out is about 150 or more, owing to longer MD trajectories. Thus, we have at least 300 distinct isomers for each system. It has been confirmed by vibrational analysis that these are indeed local minima. Figure 4 summarizes the whole isomer analysis. The top-most part of Fig. 4 shows some selected isomers. Isomers with same structural motif as that of GS, but with one or two displaced atoms are termed as "class I" isomers. The class I isomers with same structure for Al_{36} and Ga_{36} are shown in blue color. Atom indicated

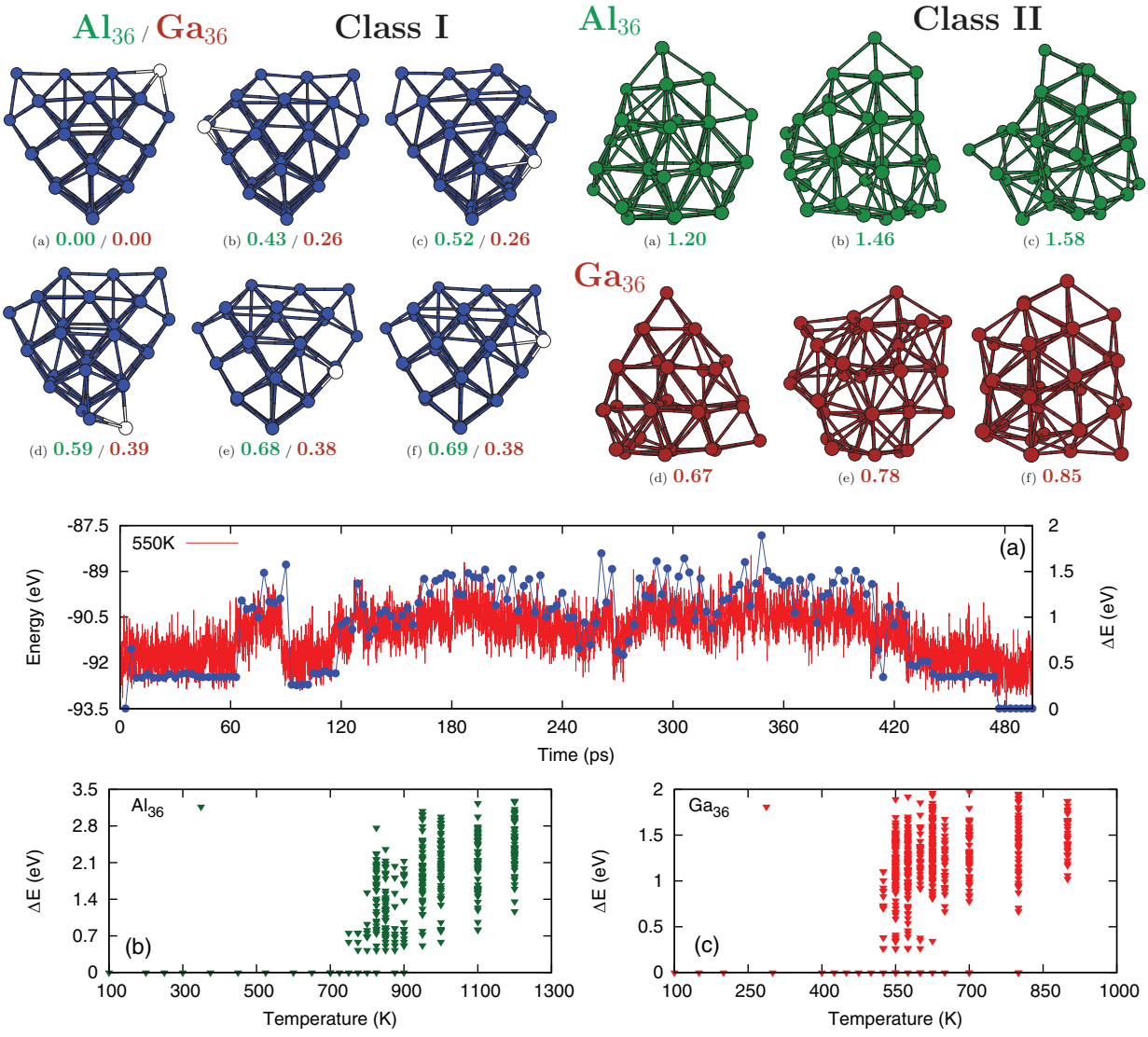

FIG. 4. Top (left): Isomers shown in blue are named as "class I" isomers having same structural motif as that of GS. The white atom indicates the displaced atom. Top (right): Isomers shown in green are high energy isomers for Al_{36} and that of Ga_{36} are shown in red. The numbers at base represent difference in energy with respect to the GS energy in eV. The top box (tagged as (a)) represents the potential energy as a function of time for Ga_{36} at 550 K (red line). The blue dots in the same box represent the isomers obtained by local optimization and the respective energies are plotted with reference to GS energy. The next two plots (tagged as (b) and (c)) represent distribution of isomers at different temperatures.

by white color represents displaced atom compared to the GS structure. The energy difference with respect to the GS (ΔE measured in eV), is shown at the base. It is instructive to note that, the 1st isomer appears at 0.26 eV above the GS in case of Ga_{36}, and for Al_{36}, the corresponding ΔE is 0.43 eV. Further, ΔE depends upon the position of the displaced atom. For Ga_{36}, the energy barrier does not depend much on whether the displaced atom resides on the nearest surface or at the nearest position. However, same situation in case of Al_{36} costs more energy as can be seen from energies shown for class I isomers in the figure. This brings out a subtle difference between these two systems. For Ga_{36}, once the initial barrier is crossed it does not require more energy to hop from one site to other on the same surface. For Al_{36}, hopping from one site to another on the same surface also requires energy of the order of 0.1 eV. The class II isomers, which are high energy isomers, have completely different structural motif than that of the GS. For Ga_{36}, the first isomer from this class appears at 0.67 eV higher than the GS (shown in Fig. 4). For Al_{36}, the first isomer belonging to this isomer family (class II) appears at 1.2 eV higher than the GS. (shown in Fig. 4). Figure 4(a) represents a typical potential energy sampling (shown in red color) at a specific temperature (in this case 550 K) for Ga_{36}. At this temperature, the isomerization is evident from the graph. The energies of optimized geometries (selected from the same MD trajectory) with respect to the GS energy are shown by dots (blue in color). It is interesting to note that the cluster is excited to a higher energy isomer from its GS, and then visits the isomers which have same structural motif. This is observed for all the higher temperatures for Ga_{36} as well as for Al_{36}. Next, two boxes in Figs. 4(b) and 4(c) refer to isomer energies (ΔE) as a function of temperature. Note that, for Al_{36}, the isomerization begins at 750 K, whereas for Ga_{36}, the first isomer appears at 525 K. In case of Ga_{36}, both families of isomers are accessible at 525 K whereas for Al_{36}, up to 800 K, dominant isomers belong to class-I. These observations are consistent with the δ_{rms}, where the sharp rise was observed for these temperatures due to initiation of isomerization. Another interesting observation is that when the cluster is in "liquid-like" state, most of the isomers are class II isomers. Probability of system visiting GS or class I isomers is much less in liquid like state. Thus, from the isomer distribution one infers about the transition temperatures. For Al_{36}, the transition region is 750 K to 900 K, whereas it is 525 K to 600 K for Ga_{36}. Note that, for Al_{36}, the width of the transition region is almost double of that Ga_{36}. These observations are also consistent with the heat capacity curve of these two systems.

In Fig. 5, isomer energies are plotted for three temperatures from the transition region. The initial geometries for these optimizations were picked up (equidistant and unbiased) from the transition temperature MD data. Hence, the x-axis also represents the time scale. Specifically, the initial structure of *n*th isomer is picked up after 3n ps of MD simulation. For Al_{36} (see Fig. 5(a)), the selected temperatures are 800 K, 825 K, and 850 K. As has been noted previously, although the isomerization begins at 750 K for Al_{36}, up to 800 K, class I isomers (ΔE < 1.0 eV) are dominantly observed, which is evident from the figure (shown with green dots in Fig. 5(a)). With increasing temperature, class I isomers become less probable and at 850 K, most of the isomers belong to class-II (shown with red dots in Fig. 5(a)). In case of Ga_{36} at 525 K, both types of isomer families are present. However, high energy (or class-II) isomers are observed with much larger simulation times (in this case after 450 ps). At higher temperatures class-II isomers are more frequent. Thus, the isomer analysis is crucial in understanding the finite temperature behavior of the cluster.

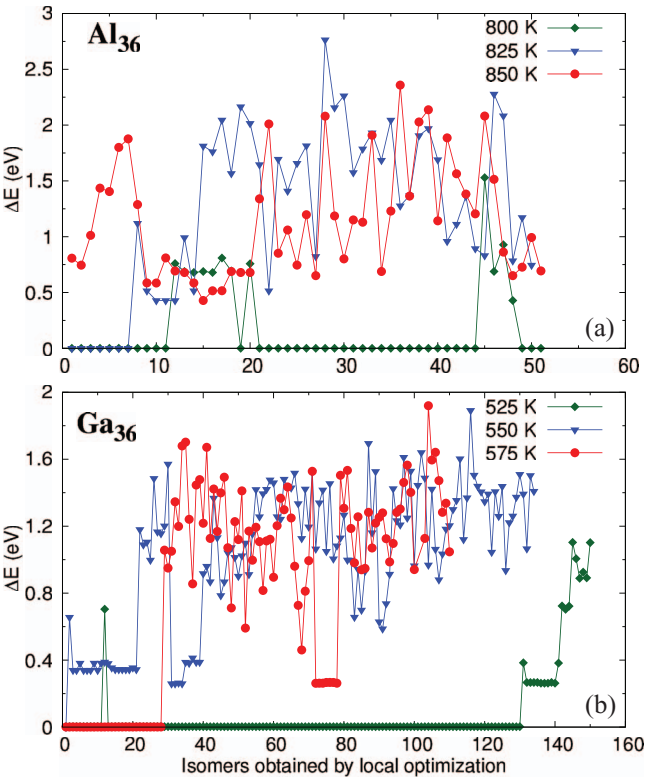

FIG. 5. Isomers obtained by local optimization for the temperatures in the transition region for Al_{36} (top) and Ga_{36} (bottom).

IV. CONCLUSIONS

Here, we report finite temperature analysis of two clusters Al_{36} and Ga_{36} having identical ground state motif and number of valence electrons. We have simulated the finite temperature behavior of these two clusters by employing Born-Oppenheimer molecular dynamics simulations to understand effect of the similar structural motif on the finite temperature behavior of the cluster. The detailed isomer analysis has been carried out, which reveals that isomers which are more probable before cluster melts have striking similarities and do have strong influence of the GS structure. Based on the appearance of various isomers, transition region could be determined for Ga_{36}, between 525 K and 600 K and for Al_{36}, between 750 K and 900 K. Further, liquid state can also be characterized by absence of class I isomers.

ACKNOWLEDGMENTS

Computational facility from CMMACS-Bangalore, CDAC-Pune, and IUAC-Delhi is gratefully acknowledged. Authors acknowledge COE-SPIRIT and COESC for partial

financial support. Authors thank V. Kaware for fruitful discussions. A.S. acknowledges CSIR for fellowship.

[1]G. A. Breaux, B. Cao, and M. F. Jarrold, "Second-order phase transitions in amorphous gallium clusters," J. Phys. Chem. B **109**, 16575 (2005).
[2]H.-P. Cheng, X. Li, R. L. Whetten, and R. S. Berry, "Complete statistical thermodynamics of the cluster solid-liquid transition," Phys. Rev. A **46**, 791 (1992).
[3]R. E. Kunz and R. S. Berry, "Coexistence of multiple phases in finite systems," Phys. Rev. Lett. **71**, 3987 (1993).
[4]D. J. Wales and R. S. Berry, "Coexistence in finite systems," Phys. Rev. Lett. **73**, 2875 (1994).
[5]A. Proykova and R. S. Berry, "Insights into phase transitions from phase changes of clusters," J. Phys. B: At. Mol. Opt. Phys. **39**, R167 (2006).
[6]H.-P. Cheng and R. S. Berry, "Surface melting of clusters and implications for bulk matter," Phys. Rev. A **45**, 7969 (1992).
[7]Z. B. Güvenç and J. Jellinek, "Surface melting in Ni_{55}," Z. Phys. D: At., Mol. Clusters **26**, 304 (1993).
[8]C. Hock, C. Bartels, S. Straßburg, M. Schmidt, H. Haberland, B. von Issendorff, and A. Aguado, "Premelting and postmelting in clusters," Phys. Rev. Lett. **102**, 043401 (2009).
[9]F. Calvo and F. Spiegelman, "On the premelting features in sodium clusters," J. Chem. Phys. **120**, 9684 (2004).
[10]M. Schmidt, B. von Issendorff, R. Kusche, and H. Haberland, "Irregular variations in the melting point of size-selected atomic clusters," Nature (London) **393**, 238 (1998).
[11]M. Schmidt and H. Haberland, "Phase transitions in clusters," C. R. Phys. **3**, 327 (2002).
[12]C. M. Neal, A. K. Starace, and M. F. Jarrold, "Ion calorimetry: Using mass spectrometry to measure melting points," J. Am. Soc. Mass Spectrom. **18**, 74 (2007).
[13]G. A. Breaux, R. C. Benirschke, T. Sugai, B. S. Kinnear, and M. F. Jarrold, "Hot and solid gallium clusters: Too small to melt," Phys. Rev. Lett. **91**, 215508 (2003).
[14]G. A. Breaux, D. A. Hillman, C. M. Neal, R. C. Benirschke, and M. F. Jarrold, "Gallium cluster 'Magic Melters'," J. Am. Chem. Soc. **126**, 8628 (2004).
[15]G. A. Breaux, C. M. Neal, B. Cao, and M. F. Jarrold, "Melting, premelting, and structural transitions in size-selected aluminum clusters with around 55 atoms," Phys. Rev. Lett. **94**, 173401 (2005).
[16]C. M. Neal, A. K. Starace, and M. F. Jarrold, "Melting transitions in aluminum clusters: The role of partially melted intermediates," Phys. Rev. B **76**, 054113 (2007).
[17]A. K. Starace, B. Cao, C. M. Neal, A. Aguado, M. F. Jarrold, and J. M. López, "Electronic effects on melting: Comparison of aluminum cluster anions and cations," J. Chem. Phys. **131**, 044307 (2009).
[18]A. Aguado and J. López, "Electronic shell and dynamical coexistence effects in the melting of aluminum clusters: An interpretation of the calorimetric experiments through computer simulation," J. Phys. Chem. Lett. **4**, 2397 (2013).
[19]S. Chacko, D. G. Kanhere, and S. A. Blundell, "First principles calculations of melting temperatures for free Na clusters," Phys. Rev. B **71**, 155407 (2005).
[20]S. M. Ghazi, S. Zorriasatein, and D. G. Kanhere, "Building clusters atom-by-atom: From local order to global order," J. Phys. Chem. A **113**, 2659 (2009).
[21]S. Chacko, K. Joshi, D. G. Kanhere, and S. A. Blundell, "Why do gallium clusters have a higher melting point than the bulk?," Phys. Rev. Lett. **92**, 135506 (2004).
[22]A. Susan, V. Kaware, A. Kibey, and K. Joshi, "Correlation between the variation in observed melting temperatures and structural motifs of the global minima of gallium clusters: An *ab initio* study," J. Chem. Phys. **138**, 014303 (2013).
[23]M.-S. Lee and D. G. Kanhere, "Effects of geometric and electronic structure on the finite temperature behavior of Na_{58}, Na_{57}, and Na_{55} cluster," Phys. Rev. B **75**, 125427 (2007).
[24]K. Joshi, S. Krishnamurty, and D. G. Kanhere, "'Magic Melters' have geometrical origin," Phys. Rev. Lett. **96**, 135703 (2006).
[25]S. Krishnamurty, D. G. Kanhere, G. S. Shafai, B. Soulé de Bas, and M. J. Ford, "*Ab initio* molecular dynamical investigation of the finite temperature behavior of the tetrahedral Au_{19} and Au_{20} clusters," J. Phys. Chem. A **111**, 10769 (2007).
[26]S. M. Ghazi, M.-S. Lee, and D. G. Kanhere, "The effects of electronic structure and charged state on thermodynamic properties: an *ab initio* molecular dynamics investigations on neutral and charged clusters of Na_{39}, Na_{40}, and Na_{41}," J. Chem. Phys. **128**, 104701 (2008).
[27]J. Kang, S.-H. Wei, and Y.-H. Kim, "Origin of the diverse melting behaviors of intermediate-size nanoclusters: Theoretical study of Al_N (N = 51-58, 64)," J. Am. Chem. Soc. **132**, 18287 (2010).
[28]H. Haberland, T. Hippler, J. Donges, O. Kostko, M. Schmidt, and B. von Issendorff, "Melting of sodium clusters: Where do the magic numbers come from?," Phys. Rev. Lett. **94**, 035701 (2005).
[29]M.-S. Lee, S. Chacko, and D. G. Kanhere, "First-principles investigation of finite-temperature behavior in small sodium clusters," J. Chem. Phys. **123**, 164310 (2005).
[30]A. Aguado, "Stepwise melting in Na_{41}^+: A first-principles critical analysis of available experimental results," J. Phys. Chem. C **115**, 13180 (2011).
[31]J. Kang and Y.-H. Kim, "Half-solidity of tetrahedral-like Al_{55} clusters," ACS Nano **4**, 1092 (2010).
[32]K. G. Steenbergen and N. Gaston, "First-principles melting of gallium clusters down to nine atoms: structural and electronic contributions to melting," Phys. Chem. Chem. Phys. **15**, 15325 (2013).
[33]K. G. Steenbergen, D. Schebarchov, and N. Gaston, "Electronic effects on the melting of small gallium clusters," J. Chem. Phys. **137**, 144307 (2012).
[34]J. M. Vásquez-Pérez, P. Calaminici, and A. M. Köster, "Heat capacities from Born-Oppenheimer molecular dynamics simulations: Al_{27}^+, Al_{28}^+," Comput. Theor. Chem. **1021**, 229 (2013).
[35]K. G. Steenbergen and N. Gaston, "Geometrically induced melting variation in gallium clusters from first principles," Phys. Rev. B **88**, 161402 (2013).
[36]C. M. Neal, A. K. Starace, M. F. Jarrold, K. Joshi, S. Krishnamurty, and D. G. Kanhere, "Melting of aluminum cluster cations with 31-48 atoms: experiment and theory," J. Phys. Chem. C **111**, 17788 (2007).
[37]S. Krishnamurty, S. Chacko, D. G. Kanhere, G. A. Breaux, C. M. Neal, and M. F. Jarrold, "Size-sensitive melting characteristics of gallium clusters: Comparison of experiment and theory for Ga_{17}^+ and Ga_{20}^+," Phys. Rev. B **73**, 045406 (2006).
[38]S. Krishnamurty, S. Zorriasatein, K. Joshi, and D. G. Kanhere, "Density functional analysis of the structural evolution of Ga_n (n = 30–55) clusters and its influence on the melting characteristics," J. Chem. Phys. **127**, 054308 (2007).
[39]K. Joshi, D. G. Kanhere, and S. A. Blundell, "Thermodynamics of tin clusters," Phys. Rev. B **67**, 235413 (2003).
[40]A. K. Starace, B. Cao, C. M. Neal, M. F. Jarrold, and A. Aguado, "Correlation between the latent heats and cohesive energies of metal clusters," J. Chem. Phys. **129**, 144702 (2008).
[41]S. Nunez, J. M. Lopez, and A. Aguado, "Neutral and charged gallium clusters: structures, physical properties and implications for the melting features," Nanoscale **4**, 6481 (2012).
[42]X. G. Gong, G. L. Chiarotti, M. Parrinello, and E. Tosatti, "α-gallium: A metallic molecular crystal," Phys. Rev. B **43**, 14277 (1991).
[43]N. Drebov, F. Weigend, and R. Ahlrichs, "Structures and properties of neutral gallium clusters: A theoretical investigation," J. Chem. Phys. **135**, 044314 (2011).
[44]G. Kresse and J. Furthmüller, "Efficient iterative schemes for *ab initio* total-energy calculations using a plane-wave basis set," Phys. Rev. B **54**, 11169 (1996).
[45]G. Kresse and D. Joubert, "From ultrasoft pseudopotentials to the projector augmented-wave method," Phys. Rev. B **59**, 1758 (1999).
[46]G. Kresse and J. Furthmüller, "Efficiency of *ab initio* total energy calculations for metals and semiconductors using a plane-wave basis set," Comput. Mater. Sci. **6**, 15 (1996).
[47]G. Kresse and J. Hafner, "*Ab initio* molecular-dynamics simulation of the liquid-metal-amorphous-semiconductor transition in germanium," Phys. Rev. B **49**, 14251 (1994).
[48]P. E. Blöchl, "Projector augmented-wave method," Phys. Rev. B **50**, 17953 (1994).
[49]J. P. Perdew, K. Burke, and M. Ernzerhof, "Generalized gradient approximation made simple," Phys. Rev. Lett. **77**, 3865 (1996); **78**, 1396 (1997).
[50]L. Ma, B. von Issendorff, and A. Aguado, "Photoelectron spectroscopy of cold aluminum cluster anions: Comparison with density functional theory results," J. Chem. Phys. **132**, 104303 (2010).
[51]P. Chandrachud, K. Joshi, and D. G. Kanhere, "Thermodynamics of carbon-doped Al and Ga clusters: *Ab initio* molecular dynamics simulations," Phys. Rev. B **76**, 235423 (2007).
[52]D. G. Kanhere, A. Vichare, and S. A. Blundell, *Reviews in Modern Quantum Chemistry* (World Scientific, Singapore, 2001).